arXiv:1002.4412v1 [astro-ph.SR] 23 Feb 2010

A NLTE analysis of boron abundances in metal-poor stars*

Kefeng Tan[1,2], Jianrong Shi[1], and Gang Zhao[1]

ABSTRACT

The non-local thermodynamic equilibrium (NLTE) line formation of neutral boron in the atmospheres of cool stars are investigated. Our results confirm that NLTE effects for the B I resonance lines, which are due to a combination of overionization and optical pumping effects, are most important for hot, metal-poor, and low-gravity stars; however, the amplitude of departures from LTE found by this work are smaller than that of previous studies. In addition, our calculation shows that the line formation of B I will get closer to LTE if the strength of collisions with neutral hydrogen increases, which is contrary to the result of previous studies. The NLTE line formation results are applied to the determination of boron abundances for a sample of 16 metal-poor stars with the method of spectrum synthesis of the B I 2497 Å resonance lines using the archived *HST*/GHRS spectra. Beryllium and oxygen abundances are also determined for these stars with the published equivalent widths of the Be II 3131 Å resonance and O I 7774 Å triplet lines, respectively. The abundances of the nine stars which are not depleted in Be or B show that, no matter the strength of collisions with neutral hydrogen may be, both Be and B increase with O quasi-linearly in the logarithmic plane, which confirms the conclusions that Be and B are mainly produced by primary process in the early Galaxy. The most noteworthy result of this work is that B increases with Fe or O at a very similar speed as, or a bit faster than Be does, which is in accord with the theoretical models. The B/Be ratios remain almost constant over the metallicity range investigated here. Our average B/Be ratio falls in the interval [$13\pm4, 17\pm4$], which is consistent with the predictions of spallation process. The contribution of B from the ν-process may be required if the ^{11}B/^{10}B isotopic ratios in metal-poor stars are the same as the

---

[*] Based on observations made with ESO telescopes and NASA/ESA *Hubble Space Telescope* obtained from the ESO/ST-ECF Science Archive Facility; based on spectral data retrieved from the ELODIE archive at Observatoire de Haute-Provence (OHP).

[1] Key Laboratory of Optical Astronomy, National Astronomical Observatories, Chinese Academy of Sciences, Beijing 100012, China; [tan, sjr, gzhao]@bao.ac.cn

[2] Graduate University of Chinese Academy of Sciences, Beijing 100049, China

meteoric value. An accurate measurement of the ^{11}B/^{10}B ratios in metal-poor stars is crucial to understanding the production history of boron.

Subject headings: Galaxy: evolution — line: formation — line: profiles — stars: abundances — stars: atmospheres — stars: Population II

1. Introduction

The origin and evolution of boron (and beryllium) are of special interest because they are hardly produced by the standard big bang nucleosynthesis (BBN), nor can they be produced by nuclear fusions in stellar interiors. Reeves et al. (1970) were the first to propose that most of the light elements (Li, Be, and B) can be produced by the high energy processes involving Galactic cosmic rays (GCR) acting on the interstellar medium (ISM). Subsequent detailed model by Meneguzzi et al. (1971) could reproduce most of the observations at that time; one of the exceptions is that the theoretical isotopic abundance ratio ^{11}B/^{10}B[1] (2.4) is lower than the observed solar meteoritic value of about 4.0. In order to solve this problem, they introduced a non-observable intense low energy component to the GCR. Woosley et al. (1990) proposed that ^{7}Li and ^{11}B can be synthesized by neutrino spallation in the helium and carbon shells of supernovae, i.e., the so-called ν-process, which argues against the existence of an unobserved low energy component of GCR. Nevertheless, the GCR process, which predicts a quadratic relation between B (also Be) and O abundances, remained as the standard picture for light elements production until the late 1980's. However, later observations on B (Duncan et al. 1992; Edvardsson et al. 1994; Duncan et al. 1997, 1998b; García López et al. 1998), as well as on Be in metal-poor stars showed that B and Be abundances increase quasi-linearly with O abundances, which indicates that B and Be are probably produced by primary process, rather than the standard secondary GCR process.

All the studies on B abundances mentioned above were based on the ultraviolet (UV) B I resonance lines at 2497 Å. Kiselman (1994, hereafter K94) investigated the formation of the B I resonance lines in the atmospheres of solar-type stars and found significant departures from LTE in stars hotter or more metal-deficient than the Sun. In their subsequent work, Kiselman & Carlsson (1996, hereafter KC96) presented the NLTE abundance corrections for the B I 2497 Å resonance lines for a grid of cool stellar model atmospheres. After that, in almost all the studies on boron, B abundances were determined in LTE first and then corrected with the results of KC96. However, NLTE corrections are model dependent and in principle should be applied only to the analysis using the same model atmospheres. Moreover, Boesgaard et al. (2004) pointed that B abundance with the NLTE corrections of KC96 increases more slowly for halo stars than the Be abundance does, which is not predicted by light-element synthesis or depletion, therefore they suggested a full NLTE analysis for B, rather than simply applying corrections to the LTE abundances.

---

[1] A/B = N(A)/N(B)

The aim of this work is thus to re-investigate the NLTE line formation of neutral boron in the atmospheres of cool stars first, and then to obtain the NLTE B abundances for a sample of metal-poor stars, based on which the origin and evolution of B in the early Galaxy can be investigated. In § 2 we briefly describe the observations and data reduction. Section 3 presents the adopted model atmospheres and stellar parameters. Section 4 deals with the NLTE line formation of neutral boron. Section 5 gives the abundances and uncertainties. In § 6 we discuss the implications for the origin and evolution of boron, while in the last section we briefly summarize our results and conclusions.

2. Observations and data reduction

Our analysis of B abundances are based on the archived spectra of 16 cool metal-poor stars ($-2.7 < \mathrm{[Fe/H]}^2 < -0.5$), which were obtained with the Goddard High Resolution Spectrograph (GHRS) on board the *Hubble Space Telescope* (*HST*). The sample stars were selected from four original studies on boron abundances (Duncan et al. 1992, 1997; García López et al. 1998; Primas et al. 1999). All the stars were observed using the G270M grating centered at the B I 2497 Å resonance doublet with a resolution of about 25,000. The signal-to-noise ratios (S/N) of the spectra are higher than 50 per diode. More details about the observations can be retrieved from the *HST* Science Archive Database and the aforementioned original paper. The spectra were reduced following the standard *HST* procedure using the STSDAS package of the IRAF[3] suite of programs.

---

[2] $\mathrm{[A/B]} = \log[N(\mathrm{A})/N(\mathrm{B})]_\bigstar - \log[N(\mathrm{A})/N(\mathrm{B})]_\odot$

[3] IRAF is distributed by the National Optical Astronomy Observatories, which are operated by the Association of Universities for Research in Astronomy, Inc., under cooperative agreement with the National Science Foundation.

3. Model atmospheres and stellar parameters

We adopted the opacity sampling (OS) model atmosphere MAFAGS-OS9 presented by Grupp et al. (2009) both in the NLTE line formation investigation and in the abundance analysis. This model is based on the one-dimensional (1D) LTE theoretical model atmosphere MAFAGS-OS described by Grupp (2004) but incorporates the Kurucz (2009) iron atomic data as well as the new bound-free (b-f) opacities for Mg I and Al I. The emergent solar flux from this new model shows significantly better agreement with observations, especially in the UV region of the spectrum, as can be seen in Figure 3 of Grupp et al. (2009).

Stellar parameters are fundamental to deriving elemental abundances in the photospheres of stars. However, it's impractical to determine them accurately with the narrow-wavelength-range (about 40 Å) and severely-blended UV *HST*/GHRS spectra. We noted that 11 of our sample stars had been studied previously by Korn et al. (2003), Gehren et al. (2006), Mashonkina et al. (2008), and Tan et al. (2009), where the stellar parameters were determined spectroscopically using almost the same model atmosphere code and technique, i.e., effective temperatures were derived by fitting the wings of Balmer lines; surface gravities were based on the *Hipparcos* parallaxes (Perryman et al. 1997) if available[4]; iron abundances were determined from Fe II lines; and the microturbulent velocities were estimated by requiring the iron abundances independent of equivalent widths or by fitting the strongest Fe II, Ca I, and Mg I lines which are sensitive to microturbulent velocities. For the rest five stars, fortunately, high-resolution and high S/N spectra covering a wide wavelength range were available from the archived ESO VLT/UVES (Dekker et al. 2000) or OHP ELODIE (Moultaka et al. 2004) spectra database. In order to keep our analysis consistent, we determined the stellar parameters of these five stars using the method described above. The final stellar parameters are given in Table 1. As discussed in Tan et al. (2009), the typical uncertainties for the effective temperature, surface gravity, iron abundance, and microturbulent velocity are estimated to be ±80 K, ±0.15 dex, ±0.08 dex, and $\pm0.2\,\mathrm{km\,s^{-1}}$ respectively.

4. NLTE line formation of neutral boron

4.1. Boron atomic model

The boron atomic model adopted in this work is illustrated by its Grotrian diagram as shown in Figure 1. Details for each item, as well as a comparison with the counterpart of

---

[4] Only one star BD −13°3442 has no *Hipparcos* parallax data; its surface gravity was determined from the ionization balance between Ca I and Ca II by Mashonkina et al. (2008).

K94 are described in the following paragraphs.

4.1.1. Energy levels

The energy levels were taken from the laboratory data compiled by Kramida & Ryabtsev (2007). Fine structure splitting was neglected except for the ground state 2p ^{2}P^o. The final model atom includes 33 B I bound levels plus the B II ground state as the continuum. In fact, for testing purpose, we have extended our model by adding 61 B II bound levels and the B III ground state as the continuum, but the calculated results showed that there are no essential differences. The final boron atomic model adopted by K94 includes 30 bound levels and one continuum level, which is comparable to that of this work. The energy levels of K94 were taken from the laboratory data compilation of Bashkin & Stoner (1978) except for the higher ^{2}P^o levels which were taken from the TOPbase (Cunto et al. 1993). The mixing of laboratory and theoretical data makes the energy level sequence of K94 a bit different from that of this work, for example, their 7s ^{2}S level is higher than 7p ^{2}P^o, and the 8s ^{2}S level is higher than 8p ^{2}P^o, which are contrary to that of Kramida & Ryabtsev (2007).

4.1.2. Radiative transitions

Oscillator strengths were extracted from the TOPbase except for the transitions 2p ^{2}P^o–3s ^{2}S and 2p ^{2}P^o–2p^2 ^{2}D, which have accurate laboratory data from Johansson et al. (1993). K94 adopted exactly the same data as ours except that they excluded the lines with $f < 0.001$ and the lines of extremely long wavelength.

Photoionization cross-sections were available from the TOPbase for 26 levels; for the rest levels (the ^{4}P and ^{2}F^o levels) hydrogenic approximations were adopted. K94 also adopted the photoionization cross-sections from the TOPbase when available, but their data for the ^{4}P level was provided by Dr. K. Berrington and the ^{2}F^o levels' cross-sections were copied directly from the ^{2}P^o levels with similar energies.

4.1.3. Collisional transitions

For electron impact excitation, the effective collision strengths were available from the R-matrix with pseudostates (RMPS) calculations of Ballance et al. (2007) for the transitions among the first 12 levels; the remaining allowed and forbidden transitions were approximated by the formulae of van Regemorter (1962) and Allen (1973), respectively. Electron impact ionization cross-sections were calculated from the classical path approximation of Seaton (1962). K94 adopted the electron impact excitation cross-sections calculated by Nakazaki & Berrington (1991) for the transitions among the first nine levels; the approximation of van Regemorter (1962) was adopted for the remaining transitions. The electron impact ionization rates of K94 were calculated from the hydrogenic approximations of Allen (1973).

Excitation and ionization induced by inelastic collisions with neutral hydrogen atoms are usually calculated using the formula of Drawin (1968, 1969) presented in the form for astrophysical applications by Steenbock & Holweger (1984). However, it has been shown by Belyaev et al. (1999, for Na I) and Belyaev & Barklem (2003, for Li I) that collision rates of the resonance transitions given by Drawin's formula are overestimated by orders of magnitude. Therefore the collision efficiency was commonly constrained by applying a scaling factor $S_{\rm H}$ to the Drawin's formula empirically, and the factor could be determined by requiring the derived abundances from different lines to be consistent (Zhao et al. 1998; Zhao & Gehren 2000). In this work, the cross-sections are computed with three different scaling factors, namely $S_{\rm H} = 0$ (no collisions with neutral hydrogen), 0.1, and 1, but as there are only two observed B I lines, and one is severely blended, we are not able to determine the final $S_{\rm H}$ value using the method described above. However, as will be discussed in § 6, the uncertainty in the strength of collisions with neutral hydrogen does not affect our final conclusions much. For K94, the cross-sections for the *b*-*f* transitions induced by collisions with neutral hydrogen were calculated according to the analytic expressions of Kunc & Soon (1991), while the bound-bound (*b*-*b*) transitions were neglected.

4.2. NLTE line formation results

The coupled radiative transfer and statistical equilibrium equations for boron were solved with a revised version of the DETAIL program (Butler & Giddings 1985) based on the accelerated lambda iteration following the efficient method described by Rybicki & Hummer (1991, 1992). In addition to the continuous background opacities, line opacities introduced by hydrogen and metal lines calculated with OS method were also taken into account in solving the equations. Lines shortward and longward of 2500 Å were extracted from the VALD database (Kupka et al. 1999) and the line list of Kurucz (1992), respectively. Please refer to Shi et al. (2008) for more details about the dealing with background opacities.

The departures from LTE for the populations of the first eight energy levels of B I and the ground state of B II calculated with different collision strengths with neutral hydrogen are shown in Figure 2 for the representative metal-poor star HD 140283 (note that, for comparison, the departure coefficients shown here is calculated with the the same stellar parameters as K94, while the final abundances of HD 140283 are determined with the stellar parameters given in Table 2). It can be seen in Figure 2a that our results confirm the conclusions of K94 that the departures from LTE for the resonance lines are due to a combination of *overionization* and *optical pumping* effects. However, the amplitude of the departures from LTE for our results (see Figure 2a) are smaller than that of K94 (c.f. Figure 4 of K94). As described in § 4.1, the main differences in the boron atomic model between K94 and this work lie in:

- excitation energies for some of the higher levels;
- number of radiative *b*-*b* transitions considered;
- photoionization cross-sections for the ^{4}P and ^{2}F^o levels;
- electron impact excitation cross-sections;
- cross-sections of ionization induced by collisions with neutral hydrogen.

The marginal differences in excitation energies and photoionization cross-sections of the higher levels cannot produce such large differences in the NLTE effects. The effects of the number of radiative *b*-*b* transitions considered was tested by excluding the transitions with $f < 0.001$ as K94 did, but calculated results showed that there were no obvious differences. The differences in NLTE effects caused by the differences in electron impact excitation cross-sections was investigated in an extreme way, i.e., calculation was performed without the electron impact processes; in this case, the departures from LTE for our results increase a bit, but still are smaller than that of K94. Lastly, we checked the influences of the hydrogen collisional ionization on the NLTE effects of B I with an elaborate routine, which enabled us to treat the hydrogen collisional excitation and ionization separately. We first fixed the strength of hydrogen collisional excitation, and then calculated the NLTE effects with two different strengths of hydrogen collisional ionization ($S_{\rm H} = 0$ and 1, respectively). As a result, only marginal differences in the NLTE effects were found, which means that hydrogen collisional ionization process plays an insignificant role in the B I line formation. Similar conclusion was also derived by K94, who found the hydrogen collisional ionization rates to be several orders of magnitude smaller than the corresponding rates due to electron collisions. In a word, it's unlikely that the large differences in the NLTE effects between K94 and this work are due to the differences in atomic model.

As pointed by K94, both the overionization and optical pumping effects are caused by the hot, non-local, ultraviolet radiation fields in the line formation regions, while the background opacities in the NLTE calculation code used by K94 were just the continuous ones, i.e., the background line opacities were not included. To compensate this defect, K94 approximated the line blanketing effects on the photoionization processes by treating the transitions at fixed rates which were calculated from a specified radiation field. These radiation fields were produced directly by the adopted model atmosphere code, which had included the line blanketing via opacity sampling. However, such approximation was not applied to the radiative *b*-*b* transitions (except for some test runs), therefore the efficiency of the pumping processes would be exaggerated. In their subsequent work, KC96 used a revised version of NLTE calculation code which allows the inclusion of spectral lines in the background opacities. As a result, the departures from LTE decreased. For example, the NLTE abundance correction ($\Delta \log \epsilon(\mathrm{B})^5 = \log \epsilon(\mathrm{B})_{\mathrm{NLTE}} - \log \epsilon(\mathrm{B})_{\mathrm{LTE}}$) for the B I 2496.771 Å resonance line decreased from 0.59 to 0.49 dex for HD 140283 after including background line opacities. However, the departures from LTE for the KC96's results are still larger than ours (as will be presented below, our NLTE B abundance correction for HD 140283 amounts only to 0.2 dex when neglecting collisions with neutral hydrogen). The NLTE calculation code used in this work has included most of the newest continuous and line opacities, while some of them (the Fe I *b*-*f* opacities of Bautista 1997 and the VALD atomic line data being the most prominent) were not available for KC96 more than one decade ago. It might be possible that KC96 used smaller background opacities than that adopted in this work and thus derived larger NLTE effects for B I.

Another difference between the results of K94 and this work worthwhile to be noted is that K94 concluded that the departures from LTE would *increase* if including the *b*-*b* inelastic collisions with neutral hydrogen. This is completely contrary to our results that the line formation of B I will get closer to LTE if the strength of collisions with neutral hydrogen increases, as can be seen clearly in Figure 2. As the role of the hydrogen collisional ionization has been shown to be insignificant, the obvious changes in the NLTE effects should be mostly due to the hydrogen collisional excitation.

Figure 3 shows the NLTE abundance corrections for the B I 2496.771 Å resonance line as a function of stellar parameters. In general, the NLTE effects are large for hot, metal-poor, and low-gravity stars. This is in agreement with the results of KC96.

---

[5] $\log \epsilon(\mathrm{X}) = \log[N(\mathrm{X})/N(\mathrm{H})] + 12$

5. Abundances and uncertainties

5.1. Boron

B abundances were derived by spectrum synthesis of the B I 2497 Å resonance doublet using the IDL/FORTRAN SIU software package developed by Dr. J. Reetz. The input line list was extracted from Duncan et al. (1998a) with minor changes. We took the weaker 2496.771 Å component as the primary abundance indicator because the stronger 2497.725 Å line is severely blended. Though the weaker line is also blended with a Co I line at 2496.708 Å, it does not have significant effect on the derived B abundance as shown by Duncan et al. (1997) and Primas et al. (1999). Finally, we determined B abundances for 12 sample stars; for the rest four stars, as reported by García López et al. (1998), a combination of high effective temperature ($T_{\rm eff} > 6000$ K) and low metallicity ([Fe/H] < -2) prevented us from obtaining accurate B abundances with the B I 2496.771 Å line, thus only upper limits were given. Figure 4 shows the observed and synthetic spectra of the B I 2497 Å resonance doublet for four program stars.

The uncertainties associated with B abundances were estimated following the same procedure described by Duncan et al. (1997). Individual errors caused by uncertainties in effective temperature, surface gravity, metallicity, microturbulent velocity, photon statistics in observed spectrum, and continuum placement (a typical value of ±2% was adopted) were added in quadrature. The B abundances and final errors are given in Table 2.

As mentioned above, B abundances of our sample stars have been studied previously by other investigators (Duncan et al. 1997; García López et al. 1998; Primas et al. 1999). Figure 5 shows the comparison of LTE B abundances between the literatures and this work for the 12 stars with determined B abundances. It can be seen that the agreement is reasonable for most of the stars. The only exception is HD 184499, for which our B abundance is 0.58 dex higher than that of Duncan et al. (1997). Such a large difference is mostly due to the different stellar parameters adopted by Duncan et al. (1997) and by this work (their effective temperature and metallicity are 120 K and 0.4 dex lower than ours, respectively). If we adopted the same stellar parameters as Duncan et al. (1997), then the difference in B abundance will decrease from 0.58 to 0.28 dex, which is comparable to the uncertainties.

5.2. Oxygen

As it is believed that boron production is related to oxygen directly, O abundance would be a preferred alternative to Fe in investigating the origin and evolution of B in the

Galaxy. There are several indicators for O abundance: the UV OH lines, the [O I] 6300 and 6363 Å forbidden lines, the O I 7774 Å triplet, and the infrared (IR) vibration-rotation OH lines, and different indicators may give different O abundances. As discussed in Nissen et al. (2002) and references therein, O abundances from the OH and O I lines are very sensitive to the adopted stellar parameters, such as the effective temperature and surface gravity; moreover, line formations in cool metal-poor stars are probably far from LTE for either the UV OH lines or the O I triplet. In contrast, [O I] forbidden lines are formed very close to LTE and O abundances from these lines are not sensitive to the adopted stellar parameters. Therefore, it is normally believed that [O I] forbidden lines are the most reliable indicators for O abundances, but the difficulty is that these lines are very weak in metal-poor dwarf and subgiant stars.

For our sample stars, in the absence of reliable data for the [O I] forbidden lines, we used the O I triplet to determine their O abundances. Based on the equivalent widths of the O I 7774 Å triplet collected from the literatures, O abundances were first calculated with $\log gf =$ 0.369, 0.223, and 0.002 from Wiese et al. (1996) in LTE. Then NLTE corrections were applied according to the results of Fabbian et al. (2009) which were calculated with new electron collisional data from Barklem (2007). We were aware that the results of Fabbian et al. (2009) were based on the MARCS models (Gustafsson et al. 2008), while our LTE O abundances were determined with the MAFAGS-OS9 models. However, we also noted that Fabbian et al. (2009) found that, when using the ATLAS9 models of Castelli & Kurucz (2003), resulting NLTE abundance corrections are very similar to that obtained using MARCS models for intermediately low metallicity ([Fe/H] > -2.5) stars. This is not unexpected because of the the similarity between ATLAS9 and MARCS models. As the MAFAGS-OS9 model used in this work is also quite similar to the MARCS model atmospheres[6], we suggest that the NLTE corrections derived by Fabbian et al. (2009) can be applied to our results too. The NLTE corrections of Fabbian et al. (2009) were calculated with two different hydrogen collisional strengths, namely $S_{\rm H} = 0$ and 1. The latter was adopted in this work because both Allende Prieto et al. (2004) and Pereira et al. (2009) found that the $S_{\rm H} = 1$ case could reproduce the solar center-to-limb variations better than $S_{\rm H} = 0$. Moreover, as stated by Fabbian et al. (2009), in the case of $S_{\rm H} = 1$, derived [O/Fe] trend becomes almost flat below [Fe/H] ~ -1, which is in better agreement with the results obtained form other O abundance indicators; and if $S_{\rm H} = 0$ is adopted, then [O/Fe] will decrease towards lower [Fe/H], which would open new questions. The final NLTE-corrected O abundances are given in Table 2

---

[6] We have made comparisons between MAFAGS-OS9 and MARCS for a set of model atmospheres across the parameter space investigated here, and results show that the temperature, electron density, and gas pressure stratifications of the MAFAGS-OS9 models are very similar to that of the MARCS models.

(the reference solar O abundance is $\log \epsilon(\mathrm{O}) = 8.77$ from Tan et al. 2009; we emphasize that the slopes of the Be(B)-O abundance relationships, which are of our primary concern, are *independent* of the choice of the reference solar O abundance).

The uncertainties of O abundances were estimated from the errors of the stellar parameters and the equivalent widths. Typical errors of ±80 K in effective temperature and ±0.15 dex in surface gravity both lead to an error of ±0.05 dex in O abundance. The uncertainties in iron abundance and microturbulent velocity nearly have no effect on O abundance. A typical error of ±3 mÅ in equivalent width corresponds to an error of ±0.04 dex. In total, the typical error of O abundance is around ±0.08 dex.

5.3. Beryllium

Beryllium abundance can be a useful tool to understand the origin and evolution of boron. It is suggested that Be is only produced by spallation reactions, while B may be additionally yielded by the ν-process, therefore, the B/Be ratio can put some constraints on the production history of B. We computed the Be abundances from the equivalent widths of the Be II 3131.066 Å resonance line ($\log gf = -0.468$ from Kurucz 1992 was adopted) given by Boesgaard & King (1993) and Boesgaard et al. (1999) for 13 of our sample stars. For the remaining three stars, Be abundances were adopted from the literatures but scaled to our stellar parameters. Beryllium abundances of all the stars were determined in LTE as NLTE effects for the Be II resonance lines are insignificant according to the results of García López et al. (1995).

The uncertainties of Be abundances mainly come from the errors of the stellar parameters and equivalent widths. The uncertainties associated with the equivalent widths, which were not given by Boesgaard & King (1993) and Boesgaard et al. (1999), depend mostly on the placement of continuum. As discussed by Duncan et al. (1997) for boron, the continuum is easier to define for more metal-poor stars, but the B lines are weaker; for stars with higher metallicity, the errors in continuum placement are larger but the B lines are stronger, so the combined effects are relatively constant over the metallicity range investigated. This situation holds also for Be. We noted that Boesgaard & King (1993) claimed a typical relative error of about 1% (in the worst cases 2%) for their continuum placement, and Boesgaard et al. (1999) estimated the typical Be abundance errors due to the placement of the continuum to be 0.02–0.06 dex. In this work, we adopted a conservative value of 0.1 dex as the typical uncertainty caused by the errors in continuum location. The Be abundances and final errors are listed in Table 2.

6. Discussion

In this section we will investigate the implications for the origin and evolution of boron from the abundances of our sample stars. Before that it is necessary to check whether some of the stars are depleted in B because B can be destroyed in stars by fusion reactions at a relatively low temperature (about 5×10^6 K). This can be done by investigating their Li and Be abundances because the destruction temperature for Li, Be, and B increases in order. If Li or Be is not depleted, then B should not be depleted either. Among the 12 stars with determined B abundances, five are very likely depleted in Li (far below the Spite plateau) according to García López et al. (1998) and Primas et al. (1999). In the following some comments are given for these Li-depleted stars:

- *HD 64090 & HD 184499*: though these two stars are obviously depleted in Li, their Be and B abundances match well with the Be-Fe(O) and B-Fe(O) trends (abundance trends in logarithmic plane, this meaning holds true for all the following denotations in the same style if not specified) determined by the Li-normal (thus Be- and B-normal) stars as can be seen in Figure 6. We conclude that their Be and B abundances are not depleted and will take them into account when investigating the origin and evolution of B.
- *HD 106516 & HD 221377*: both of them have only upper limits for their Li and Be abundances. Their B abundances are slightly lower than that of stars with similar metallicity. Primas et al. (1999) also took these two stars as possible B-depleted stars. We will exclude them in the following discussion.
- *BD +23° 3130*: this is the most metal-poor star with determined B abundance in our sample. It is possibly a giant star with $T_{\rm eff} = 5255$ K and $\log g = 2.89$. Its Be and B abundances are 0.37 and 0.25 dex lower, respectively, than that of HD 140283, which has very similar metallicity. It's hard to say whether this star is slightly depleted in Be or B, but for reliability, it will not be considered either in the following investigation.

Another star worthy of being noted is HD 160617, which was concluded as a Li-normal but B-depleted star (whether it is Be-depleted depends on the adopted stellar parameters) by Primas et al. (1998). Both the Li and Be abundances of this star determined with our stellar parameters seem to be normal (see Tan et al. 2009). Its B abundance obtained by this work is 0.24 dex higher than that of Primas et al. (1998) which was determined with very similar parameters, but considering the uncertainties, they are still in reasonable agreement. However, we do note that Be and B abundances of HD 160617 are much smaller than that of HD 64090 which has very similar Fe abundance. This large differences lead to the relatively large scatter at [Fe/H] ~ -1.8 on the Be-Fe and B-Fe trends as can be seen in Figure 6a. But on the Be-O and B-O diagram, the scatter is much smaller as shown in Figure 6b. This can be a direct evidence that Be and B production are directly related to O rather than Fe. Therefore, we take HD 160617 as a B-normal star and will include it in the following investigation on the B production and evolution. Finally, we have nine stars with normal Be and B abundances and the following discussion will be only based on these stars.

6.1. Evolution of Be and B with metal abundances

Figure 6 shows the Be and B abundances against [Fe/H] and [O/H] for the nine Be- and B-normal stars. It is obvious that both $\log \epsilon(\mathrm{Be})$ and $\log \epsilon(\mathrm{B})$ increase approximately linearly with increasing [Fe/H] or [O/H]. Slopes and intercepts for the linear leat-squares fits to the abundance data are given in Table 3; for comparison, results from previous studies are also given. It can be seen that the slope of the Be-Fe trend obtained by this work agrees well with the result of Tan et al. (2009), and is consistent with that of Smiljanic et al. (2009) within error bars. But our B-Fe trend is marginally steeper than that of Boesgaard et al. (1999) and Rich & Boesgaard (2009), which is mainly due to the different metallicity ranges investigated. When the fitting is only restricted to the similar metallicity range to this work, the slopes of the Be-Fe trends from Boesgaard et al. (1999) and Rich & Boesgaard (2009) are 1.17 and 1.07, respectively, which are consistent with our result. For the B-Fe trend, the slope obtained by this work is steeper than that of Duncan et al. (1997). This difference can be attributed to the two lowest metallicity stars (BD +3°740 and BD −13°3442) in the sample of Duncan et al. (1997), for which only upper limits of B abundances are derived by this work, and thus are not included in our investigation of the B-Fe(O) relationships. It can be seen clearly in Figure 3 of Duncan et al. (1997) that, compared with the general B-Fe trend, these two stars show obvious enhancement of B abundances, and if they are excluded from the fitting, then the slope of the B-Fe trend will increase to 1.04, which is consistent with our result within uncertainties. For the Be-O and B-O trends, comparisons become more complicated because different work may use different O abundance indicators and/or different descriptions of the line formation (LTE versus NLTE). The slope of the Be-O trend obtained by this work agrees well with the result of Tan et al. (2009), of which the O abundances were also determined using the O I triplet and had been corrected for NLTE effects. Boesgaard et al. (1999) adopted the average values of O abundances based on the UV OH lines and the O I triplet; Rich & Boesgaard (2009) determined O abundances from the UV OH lines, therefore, a direct comparison of their results with that of this work is inappropriate. Smiljanic et al. (2009) used [α/H] as a proxy for [O/H] in the absence of O abundances for all their sample stars, but interestingly, the Be-α trend obtained by them agrees well with the Be-O trend of this work. Oxygen abundances adopted by Duncan et al. (1997) for most of their sample stars were based on the O I triplet and had been corrected for NLTE effects, but for the same reason as we have mentioned in the comparison of the B-Fe trend, their B-O trend is flatter than that of this work.

Both the slopes of our Be-Fe and Be-O trends are closer to unity, which confirms the previous conclusions that Be should be mainly produced by primary process in the early Galaxy. As for B, the derived B-Fe and B-O relationships depend somehow on the adopted strength of collisions with neutral hydrogen as we have discussed in § 4.2. As shown in Figure 3b, on one side, NLTE abundance corrections will increase if the strength of collisions with neutral hydrogen decreases; on the other side, NLTE abundance corrections increases with decreasing metallicity, therefore, the $\mathrm{B_{LTE}}$-Fe(O) and $\mathrm{B_{NLTE,S_H=0}}$-Fe(O) trends shown in Figure 6 represent the two extreme cases, and the real situation should lie between them. In other words, the slopes of the B-Fe and B-O relationships should be restricted to the intervals [1.07, 1.17] and [1.34, 1.46], respectively. In any case, the slopes of the B-Fe and B-O trends are closer to 1, which indicates that primary process is dominant in B production in the early Galaxy. In addition, there seems to be slight changes in slopes for both the Be-Fe(O) and B-Fe(O) trends around [Fe/H] ~ -1 and [O/H] ~ -1, respectively, which was also reported by García López et al. (1998), but there are too few stars in our sample to confirm it.

It is believed that both Be and B can be produced by spallation reactions while B may be additionally produced by the ν-process, therefore, B should increase more rapidly than Be (or at a similar speed as Be if the contribution of the ν-process is neglectable). However, as first pointed by Boesgaard et al. (2004), after applying the NLTE abundance corrections of KC96, the B abundance increases more slowly for halo stars than Be does (see Tables 5 and 6 of Duncan et al. 1997 and Figures 11, 13, and 14 of Boesgaard et al. 2004), which is in contradiction with the theoretical models. For our results, as shown in Figure 6, this problem *no longer* exists no matter the strength of collisions with neutral hydrogen may be. Even in the extreme case (no collisions with neutral hydrogen), B increases with Fe or O at a very similar speed as Be does, and if the strength of collisions with neutral hydrogen increases, then B will increase with Fe or O a bit faster than Be. To further investigate whether our new result (B increase with Fe or O in a similar fashion to Be) are due to our smaller NLTE abundance corrections or to the LTE B abundances, we applied the NLTE abundance corrections of KC96 to our LTE B abundances. As a result, the slopes of the B-Fe and B-O trends decrease to 0.97 and 1.22, respectively, which are lower than the slopes of the Be-Fe and Be-O trends. In addition, a reverse test was also performed, i.e., we applied our NLTE corrections to the LTE B abundances of Duncan et al. (1997), and in this case, the slope of the B-Fe trend would be 0.86 (0.70 when the NLTE corrections of KC96 are applied), which is still similar to the slope of the Be-Fe trend (0.85). Therefore, our result that B increases with Fe or O at a very similar speed as Be is mostly due to the smaller NLTE abundance corrections.

Though good linear relationships between Be and Fe as well as between B and Fe are found for the metallicity range ($-2.5 <$ [Fe/H] < -0.5) investigated here, it is not clear whether such trends will continue to lower metallicities. Primas et al. (2000) reported the detection of Be in the very metal-poor star G 64–12 ([Fe/H] $= -3.3$) and found that Be abundance of this star is significantly higher than what expected from the general Be-Fe trend. This led them to suggest a possible flattening of Be abundances at very low metallicities. We also note that, for BD +3°740 and BD −13°3442, only upper limits of B abundances are found by García López et al. (1998) and by this work, while Duncan et al. (1997, 1998b) claimed the detection of B in these two stars. And interestingly, B abundances of BD +3°740 and BD −13°3442 given by Duncan et al. (1997, 1998b) also seem to be higher than what expected from the general B-Fe trend (both of these two stars are at the metallicity end of their sample). Moreover, Asplund et al. (2006) reported the detection of ^{6}Li (at the significance level $\geq 2\sigma$) in nine metal-poor stars. Their most noteworthy result is the detection of an abnormally high ^{6}Li abundance in the very metal-poor star LP 815–43, which cannot be explained either by the standard BBN or by the Galactic cosmic-ray spallation and α-fusion reactions. One common solution to all the three problems described above can be non-standard BBN, which could produce much more primordial light elements than the standard BBN. However, if ignoring the problem of high ^{6}Li abundance at very low metallicity (whether ^{6}Li is really detected in some metal-poor stars is still disputable, for example, García Pérez et al. 2009 aimed to determine ^{6}Li/^{7}Li for a sample of metal-poor stars, and only found that the ^{6}Li/^{7}Li ratios are comparable to or even lower than the associated uncertainties), there may be no need to invoke the non-standard models of BBN to explain the possible Be and B "plateau" as pointed by Vangioni-Flam et al. (1998). They proposed that in the very early Galaxy, if supernovae of all masses paly roles in the production of Be(B), then Be(B) should continue to decrease with decreasing [Fe/H]; otherwise, if only the most massive stars (initial mass larger than $60\,M_{\odot}$) contribute to the Be(B) yields, then Be(B) should be roughly constant. They suggested that the predicted difference in the behavior of Be(B) could be tested by observations at [Fe/H] ≤ -3. Recently, Rich & Boesgaard (2009) investigated the Be abundances of 24 very metal-poor stars with [Fe/H] from -2.3 to -3.5 and found changes in slopes for the Be-Fe trend at [Fe/H] ~ -2.2 as well as for the Be-O trend at [O/H] ~ -1.6. In general, their results show that Be increases with Fe(O) much more slowly below [Fe/H] ~ -2.2 ([O/H] ~ -1.6) than above that. Though there is no indication of a Be plateau, the four most metal-deficient stars ([Fe/H] < -3) do show a Be enhancement with respect to Fe at the 1σ level, which is qualitatively consistent with the predictions of the light-element production model involved with only the most massive stars proposed by Vangioni-Flam et al. (1998). To clarify this problem, more accurate data on Be and B abundances at very low metallicities are needed.

6.2. The B/Be ratio

Figure 7 shows the B/Be ratio as a function of metallicity for the nine Be and B-normal stars. Linear least-squares fits to the data give the following relationships:

$$\log\,(\mathrm{B_{LTE}/Be}) = (0.10 \pm 0.14)[\mathrm{Fe/H}] + (1.25 \pm 0.21)$$
$$\log\,(\mathrm{B_{NLTE,S_H=0}/Be}) = (0.01 \pm 0.12)[\mathrm{Fe/H}] + (1.22 \pm 0.19)$$

It is clear that, in LTE case, B/Be increases slightly with increasing metallicity, while in the case of NLTE but without neutral hydrogen collisions, B/Be is almost constant. Again, the real situation for the B/Be-Fe trend should lie between the two extreme cases, but considering the uncertainties, the B/Be ratio is roughly constant over the metallicity range investigated here. The average B/Be ratio for the nine stars should fall in the interval $[13 \pm 4, 17 \pm 4]$, of which the lower and upper limits correspond to the two extreme cases respectively. This is in reasonable agreement with the results 15 ± 3 of Duncan et al. (1997) and 20 ± 10 of García López et al. (1998). Our average B/Be ratio is consistent with the predicted value of spallation process, which depends on the compositions and energy spectra of cosmic rays (for example, a typical spallation-produced B/Be ratio of about 14 is derived by Ramaty et al. 2000). However, if assuming that B is purely produced by spallation reactions and the ^{11}B/^{10}B ratios in metal-poor stars are the same as the meteoric value, then a minimum B/Be ratio of about 20 is required (Vangioni-Flam et al. 1996). This value is slightly larger than our result, which might indicate that B is also produced by the ν-process. Ramaty et al. (2000) showed that even though the production histories of the spallation-produced B and Be and the neutrino-produced B are different, B/Be can still remain essentially constant as a function of [Fe/H]. However, the ^{11}B/^{10}B ratios in metal-poor stars need not to be the same as the meteoric value, especially considering the fact that our average B/Be ratio in metal-poor stars is lower than the solar meteoric value of about 23. Anyway, an accurate measurement of the ^{11}B/^{10}B ratios in metal-poor stars is strongly desirable.

7. Summary

In this work, we have investigated the NLTE line formation of neutral boron in the atmospheres of cool stars. Our results confirm the conclusions of K94 and KC96 that NLTE effects for the B I resonance lines, which are due to a combination of overionization and optical pumping effects, are significant for hot, metal-poor, and low-gravity stars. However, the amplitude of the departures from LTE found by the present study are smaller than that of KC96, which might be because that KC96 used smaller background opacities than that adopted in this work. In addition, our calculation shows that departures from LTE for the B I resonance lines decrease with increasing strength of collisions with neutral hydrogen, which is completely contrary to the result of K94.

The NLTE line formation results for B I have been applied to the determination of B abundances for a sample of 16 metal-poor stars, for which the Be and O abundances are also determined. No matter the strength of collisions with neutral hydrogen may be, both the slopes of the Be-O and B-O trends determined by the nine Be- and B-normal stars are closer to unity, which confirms the previous conclusions that primary process is dominant in the production of Be and B in the early Galaxy. Most importantly, our results show that, B increases with Fe or O at a very similar speed as, or a bit faster than Be does, which is in accord with the theoretical models. The B/Be abundance ratios are roughly constant over the metallicity range $-2.5 < [\mathrm{Fe/H}] < -0.5$. The average B/Be ratio falls in the interval $[13 \pm 4, 17 \pm 4]$, which is consistent with the predictions of spallation process. However, if assuming the isotopic $^{11}\mathrm{B}/^{10}\mathrm{B}$ ratios in metal-poor stars to be the same as the meteoric value, then a minimum B/Be ratio of about 20 is required by the pure spallation process, therefore the ν-process may be needed to reconcile this problem. But whether the $^{11}\mathrm{B}/^{10}\mathrm{B}$ ratios in metal-poor stars are the same as the meteoric value is still unclear, thus an accurate measurement is strongly desirable, though rather challenging.

We are grateful to Dr. Frank Grupp for providing the MAFAGS-OS9 model atmosphere code. K.T. would like to thank Dr. Martin Asplund for comments on the manuscript and suggestions on the NLTE abundance corrections for oxygen. Thanks also go to the anonymous referee for the valuable suggestions and comments. This work is supported by the National Nature Science Foundation of China under grant Nos. 10778626, 10821061, 10973016 and by the National Basic Research Program of China under grant No. 2007CB815103. This research has made use of the SIMBAD database, operated at CDS, Strasbourg, France.

REFERENCES

Akerman, C. J., Carigi, L., Nissen, P. E., Pettini, M., & Asplund, M. 2004, A&A, 414, 931

Allen, C. W. 1973, Astrophysical Quantities, (3rd ed.; London: University of London, Athlone Press)

Allende Prieto, C., Asplund, M., & Fabiani Bendicho, P. 2004, A&A, 423, 1109

Asplund, M., Lambert, D. L., Nissen, P. E., Primas, F., & Smith, V. V. 2006, ApJ, 644, 229

Ballance, C. P., Griffin, D. C., Berrington, K. A., & Badnell, N. R. 2007, J. Phys. B: At. Mol. Opt. Phys., 40, 1131

Barklem, P. S. 2007, A&A, 462, 781

Bashkin, S. & Stoner, J. O. 1978, Atomic energy levels and Grotrian Diagrams. Addenda: Hydrogen I - Phosphorus XV, (Amsterdam: North-Holland Publ. Co.)

Bautista, M. A. 1997, A&AS, 122, 167

Belyaev, A. K. & Barklem, P. S. 2003, Phys. Rev. A, 68, 2703

Belyaev, A. K., Grosser, J., Hahne, J., & Menzel, T. 1999, Phys. Rev. A, 60, 2151

Boesgaard, A. M., Deliyannis, C. P., King, J. R., Ryan, S. G., Vogt, S. S., & Beers, T. C. 1999, AJ, 117, 1549

Boesgaard, A. M. & King, J. R. 1993, AJ, 106, 2309

Boesgaard, A. M., McGrath, E. J., Lambert, D. L., & Cunha, K. 2004, ApJ, 606, 306

Butler, K. & Giddings, J. R. 1985, in Newsletter on Analysis of Astronomical Spectra No. 9 (London: University of London)

Castelli, F. & Kurucz, R. L. 2003, in IAU Symposium, Vol. 210, Modelling of Stellar Atmospheres, ed. N. Piskunov, W. W. Weiss, & D. F. Gray, 20

Cavallo, R. M., Pilachowski, C. A., & Rebolo, R. 1997, PASP, 109, 226

Cunto, W., Mendoza, C., Ochsenbein, F., & Zeippen, C. J. 1993, A&A, 275, L5

Dekker, H., D'Odorico, S., Kaufer, A., Delabre, B., & Kotzlowski, H. 2000, in SPIE Conference Series, ed. M. Iye & A. F. Moorwood, 4008, 534

Drawin, H. W. 1968, Z. Phys., 211, 404

Drawin, H. W. 1969, Z. Phys., 225, 483

Duncan, D. K., Lambert, D. L., & Lemke, M. 1992, ApJ, 401, 584

Duncan, D. K., Peterson, R. C., Thorburn, J. A., & Pinsonneault, M. H. 1998a, ApJ, 499, 871

Duncan, D. K., Primas, F., Rebull, L. M., Boesgaard, A. M., Deliyannis, C. P., Hobbs, L. M., King, J. R., & Ryan, S. G. 1997, ApJ, 488, 338

Duncan, D. K., Rebull, L. M., Primas, F., Boesgaard, A. M., Deliyannis, C. P., Hobbs, L. M., King, J. R., & Ryan, S. G. 1998b, A&A, 332, 1017

Edvardsson, B., Gustafsson, B., Johansson, S. G., Kiselman, D., Lambert, D. L., Nissen, P. E., & Gilmore, G. 1994, A&A, 290, 176

Fabbian, D., Asplund, M., Barklem, P. S., Carlsson, M., & Kiselman, D. 2009, A&A, 500, 1221

Fulbright, J. P. & Johnson, J. A. 2003, ApJ, 595, 1154

García López, R. J., Lambert, D. L., Edvardsson, B., Gustafsson, B., Kiselman, D., & Rebolo, R. 1998, ApJ, 500, 241

García López, R. J., Severino, G., & Gomez, M. T. 1995, A&A, 297, 787

García Pérez, A. E., Aoki, W., Inoue, S., Ryan, S. G., Suzuki, T. K., & Chiba, M. 2009, A&A, 504, 213

Gehren, T., Shi, J. R., Zhang, H. W., Zhao, G., & Korn, A. J. 2006, A&A, 451, 1065

Grupp, F. 2004, A&A, 420, 289

Grupp, F., Kurucz, R. L., & Tan, K. 2009, A&A, 503, 177

Gustafsson, B., Edvardsson, B., Eriksson, K., Jørgensen, U. G., Nordlund, Å. & Plez, B. 2008, A&A, 486, 951

Johansson, S. G., Litzen, U., Kasten, J., & Kock, M. 1993, ApJ, 403, L25

Jonsell, K., Edvardsson, B., Gustafsson, B., Magain, P., Nissen, P. E., & Asplund, M. 2005, A&A, 440, 321

Kiselman, D. 1994, A&A, 286, 169 (K94)

Kiselman, D. & Carlsson, M. 1996, A&A, 311, 680 (KC96)

Korn, A. J., Shi, J., & Gehren, T. 2003, A&A, 407, 691

Kramida, A. E. & Ryabtsev, A. N. 2007, Phys. Scr, 76, 544

Kunc, J. A. & Soon, W. H. 1991, J. Chem. Phys., 95, 5738

Kupka, F., Piskunov, N., Ryabchikova, T. A., Stempels, H. C., & Weiss, W. W. 1999, A&AS, 138, 119

Kurucz, R. L. 1992, Rev. Mexicana Astron. Astrofis., 23, 45

Kurucz, R. L. 2009, http://kurucz.harvard.edu/atoms/2600/, http://kurucz.harvard.edu/atoms/2601/, http://kurucz.harvard.edu/atoms/2602/

Mashonkina, L., et al. 2008, A&A, 478, 529

Meneguzzi, M., Audouze, J., & Reeves, H. 1971, A&A, 15, 337

Molaro, P., Bonifacio, P., Castelli, F., & Pasquini, L. 1997, A&A, 319, 593

Moultaka, J., Ilovaisky, S. A., Prugniel, P., & Soubiran, C. 2004, PASP, 116, 693

Nakazaki, S. & Berrington, K. A. 1991, J. Phys. B: At. Mol. Opt. Phys., 24, 4263

Nissen, P. E., Primas, F., Asplund, M., & Lambert, D. L. 2002, A&A, 390, 235

Pereira, T. M. D., Asplund, M., & Kiselman, D. 2009, A&A, 508, 1403

Perryman, M. A. C., et al. 1997, A&A, 323, L49

Primas, F., Asplund, M., Nissen, P. E., & Hill, V. 2000, A&A, 364, L42

Primas, F., Duncan, D. K., Peterson, R. C., & Thorburn, J. A. 1999, A&A, 343, 545

Primas, F., Duncan, D. K., & Thorburn, J. A. 1998, ApJ, 506, L51

Ramaty, R., Scully, S. T., Lingenfelter, R. E., & Kozlovsky, B. 2000, ApJ, 534, 747

Reeves, H., Fowler, W. A., & Hoyle, F. 1970, Nature, 226, 727

Rich, J. A. & Boesgaard, A. M. 2009, ApJ, 701, 1519

Rybicki, G. B. & Hummer, D. G. 1991, A&A, 245, 171

Rybicki, G. B. & Hummer, D. G. 1992, A&A, 262, 209

Seaton, M. J. 1962, in Atomic and Molecular Processes, ed. D. R. Bates (New York: Academic Press), 374

Shi, J. R., Gehren, T., Butler, K., Mashonkina, L. I., & Zhao, G. 2008, A&A, 486, 303

Smiljanic, R., Pasquini, L., Bonifacio, P., Galli, D., Gratton, R. G., Randich, S., & Wolff, B. 2009, A&A, 499, 103

Sneden, C., Lambert, D. L., & Whitaker, R. W. 1979, ApJ, 234, 964

Steenbock, W. & Holweger, H. 1984, A&A, 130, 319

Tan, K. F., Shi, J. R., & Zhao, G. 2009, MNRAS, 392, 205

Tomkin, J., Lemke, M., Lambert, D. L., & Sneden, C. 1992, AJ, 104, 1568

van Regemorter, H. 1962, ApJ, 136, 906

Vangioni-Flam, E., Casse, M., Fields, B. D., & Olive, K. A. 1996, ApJ, 468, 199

Vangioni-Flam, E., Ramaty, R., Olive, K. A., & Casse, M. 1998, A&A, 337, 714

Wiese, W. L., Fuhr, J. R., & Deters, T. M. 1996, Atomic transition probabilities of carbon, nitrogen, and oxygen: a critical data compilation, (Washington, DC: American Chemical Society)

Woosley, S. E., Hartmann, D. H., Hoffman, R. D., & Haxton, W. C. 1990, ApJ, 356, 272

Zhao, G., Butler, K., & Gehren, T. 1998, A&A, 333, 219

Zhao, G. & Gehren, T. 2000, A&A, 362, 1077

This preprint was prepared with the AAS LaTeX macros v5.2.

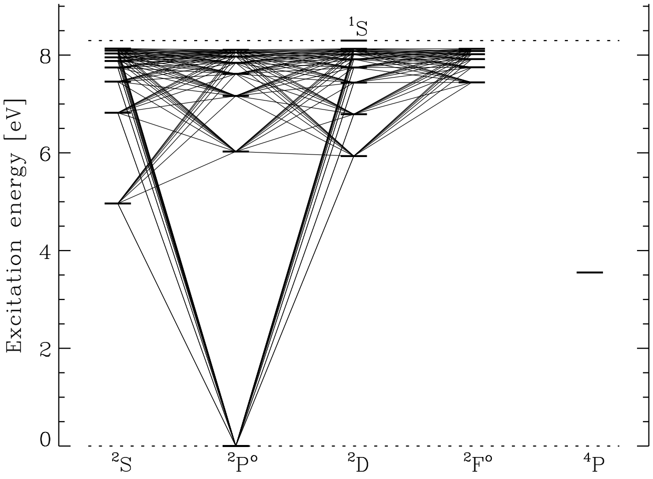

Fig. 1.— Grotrian diagram for B I (the ground state of B II is also shown). The continuous lines denote the radiative bound-bound transitions considered in this work.

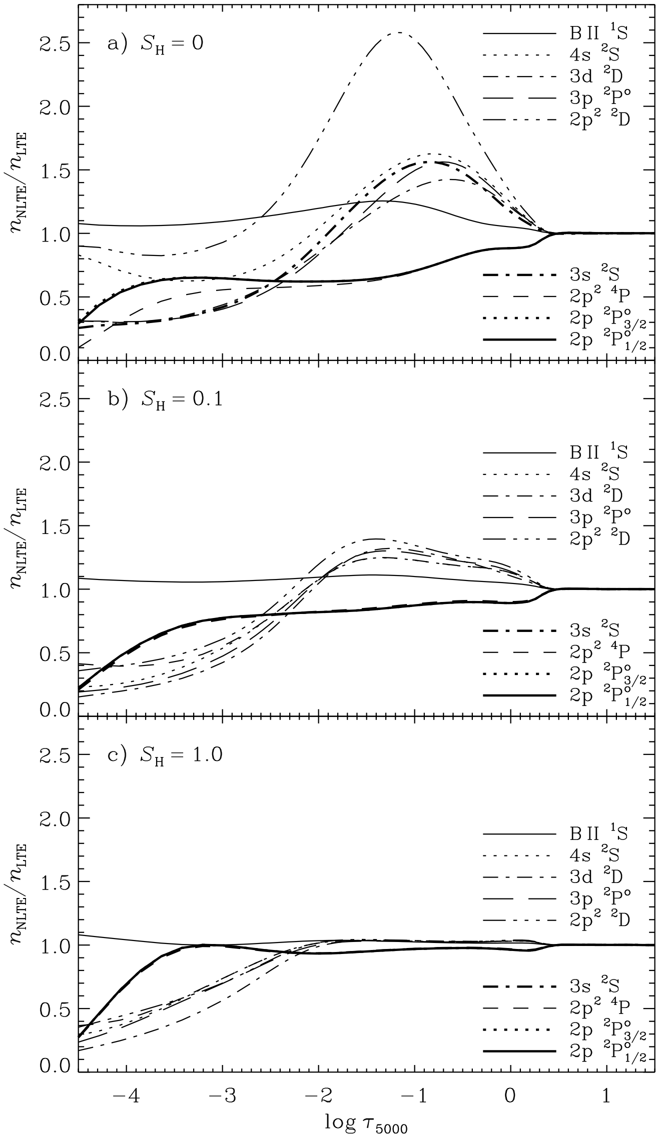

Fig. 2.— Departure coefficients for the populations of first eight energy levels of B I and the ground state of B II for the representative metal-poor star HD 140283 calculated with the stellar parameters from K94.

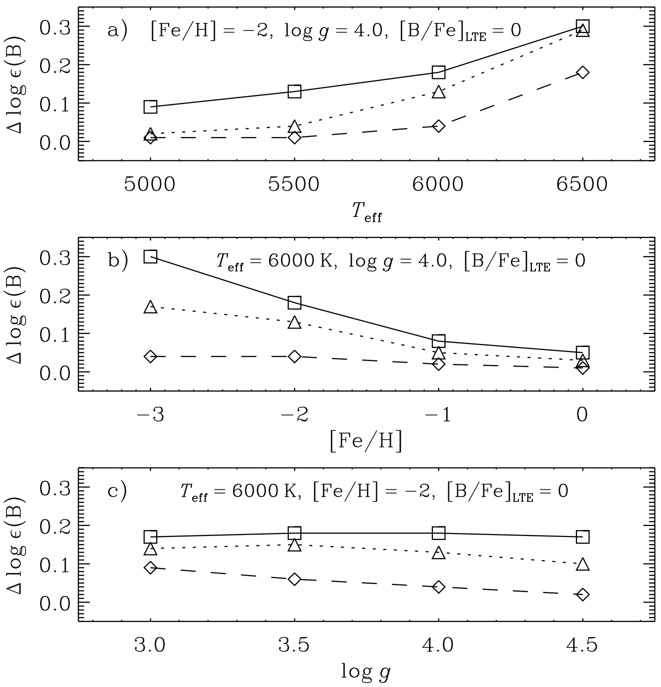

Fig. 3.— Dependence of NLTE abundance corrections for the B I 2496.771 Å resonance line on (a) effective temperature, (b) metallicity, and (c) surface gravity. Squares, triangles, and diamonds represent results calculated with different strength of collisions with neutral hydrogen, i.e., $S_{\rm H} = 0$, 0.1, and 1 respectively.

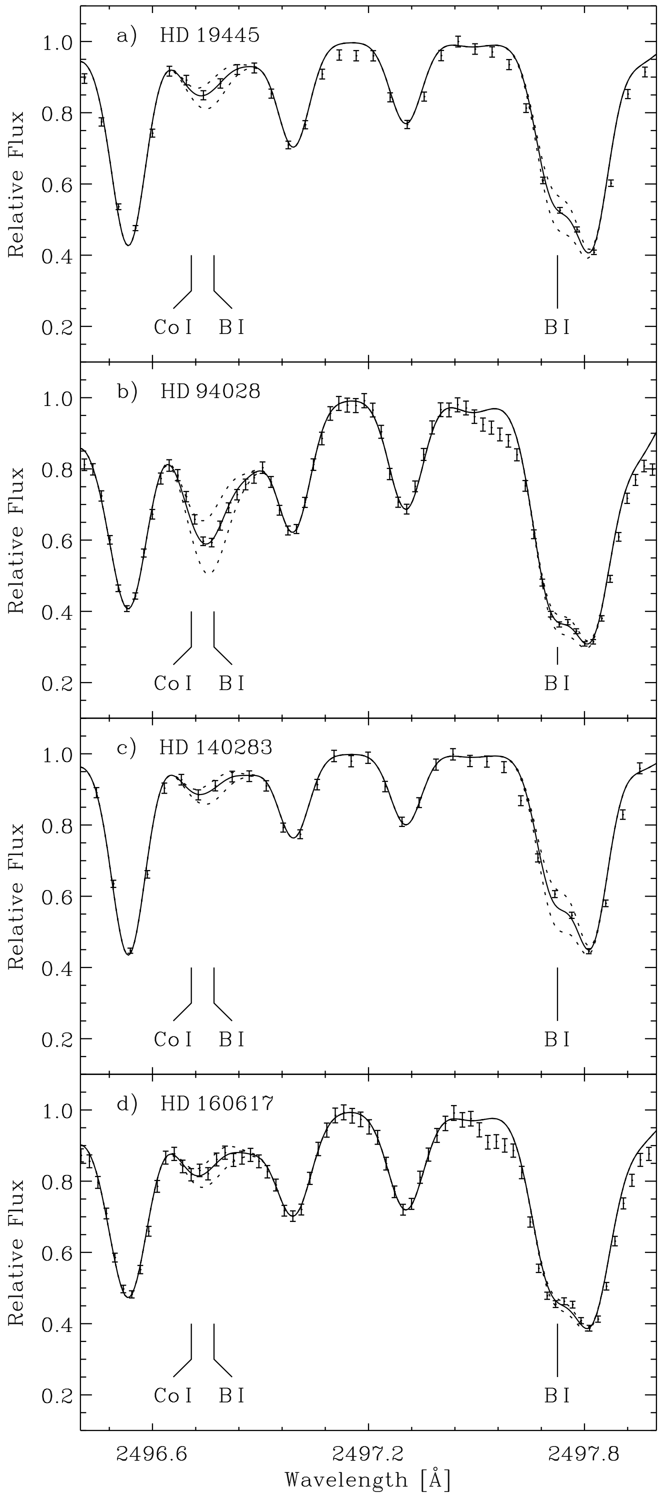

Fig. 4.— Spectrum synthesis of the B I 2497 Å resonance doublet for four program stars. The observed spectra are represented by photon statistics error bars. The solid line is the best-fitting synthesis, and the dotted lines are synthetic spectra with B abundances of ±0.2 dex relative to the best synthesis.

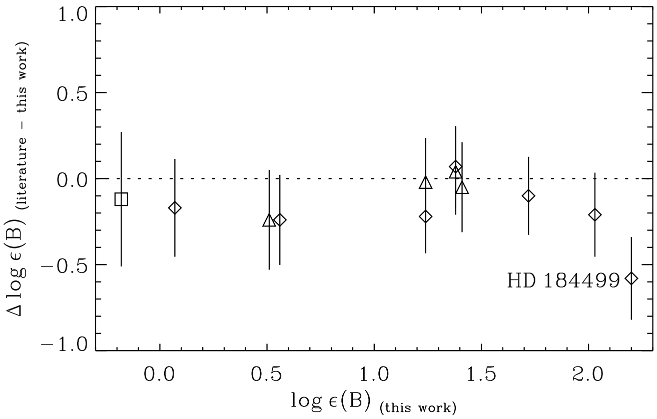

Fig. 5.— Comparison of B abundances (LTE) between the literatures and this work for the 12 stars with determined B abundances: diamonds, Duncan et al. (1997); square, García López et al. (1998); triangles, Primas et al. (1999).

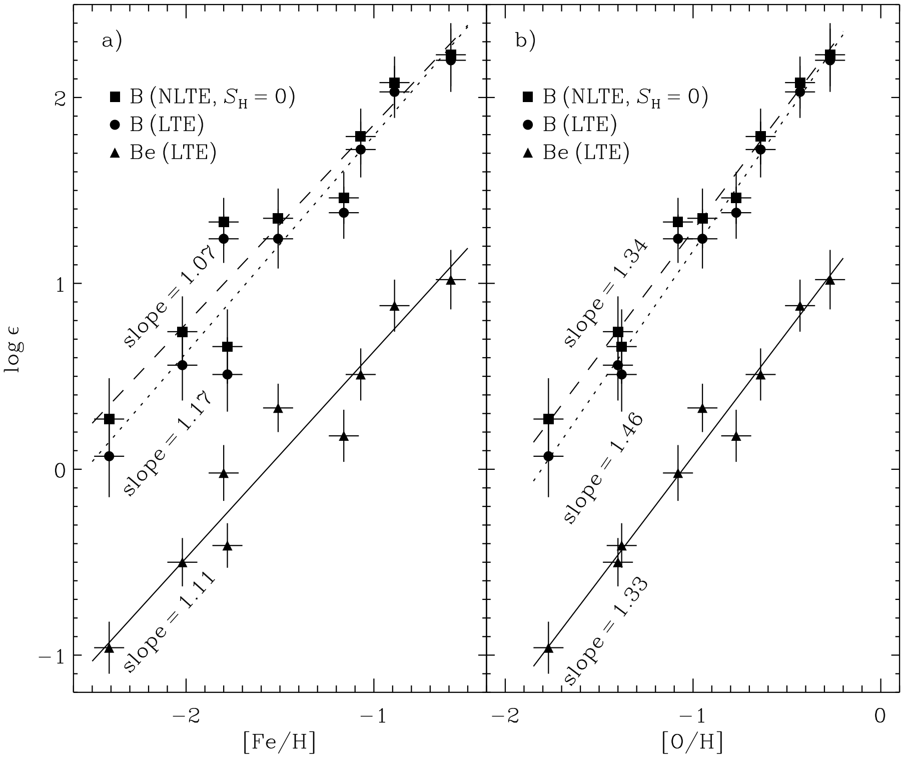

Fig. 6.— Be and B abundances against (a) [Fe/H] and (b) [O/H] for the nine Be- and B-normal stars. Filled triangles are Be abundances, filled circles are LTE B abundances, and filled squares are NLTE B abundances calculated without neutral hydrogen collisions ($S_{\mathrm{H}} = 0$). Solid, dotted, and dashed lines are the best linear fits to the Be-Fe(O), $\mathrm{B}_{\mathrm{LTE}}$-Fe(O), and $\mathrm{B}_{\mathrm{NLTE,S_H=0}}$-Fe(O) relationships respectively.

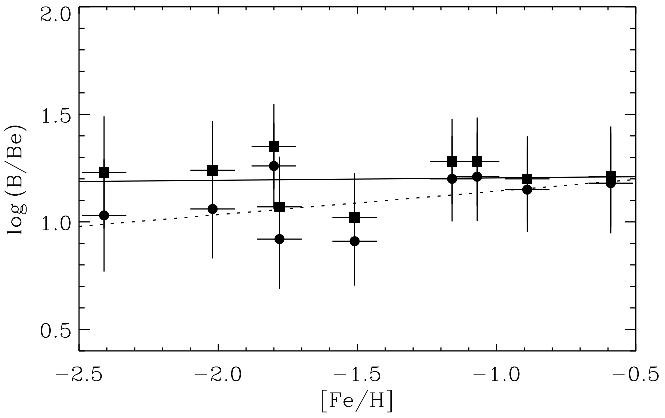

Fig. 7.— B-to-Be abundance ratio as a function of [Fe/H] for the nine Be- and B-normal stars (filled circles: B abundances calculated in LTE; filled squares: B abundances calculated in NLTE without neutral hydrogen collisions, i.e., $S_{\rm H} = 0$). Dotted and solid lines represent the best linear fits to the $\rm B_{LTE}$/Be-Fe and $\rm B_{NLTE,S_H=0}$/Be-Fe relationships, respectively.

Table 1. Stellar parameters

Star	$T_{\rm eff}$ (K)	$\log g$ (cgs)	[Fe/H] (dex)	ξ ($\rm km\,s^{-1}$)	Ref.
HD 19445	6009	4.40	−2.02	1.6	1, 2[a]
HD 64090	5525	4.57	−1.80	2.0	5
HD 76932	5890	4.12	−0.89	1.2	4
HD 84937	6356	4.00	−2.16	1.7	1, 3[a]
HD 94028	5925	4.19	−1.51	1.5	2
HD 106516	6115	4.28	−0.80	1.7	5
HD 140283	5725	3.68	−2.41	1.5	4
HD 160617	5940	3.80	−1.78	1.5	4
HD 184499	5820	4.07	−0.59	1.2	5
HD 194598	5980	4.27	−1.16	1.6	2
HD 201891	5900	4.22	−1.07	1.2	2
HD 221377	6330	3.81	−0.78	2.0	5
BD +3°740	6290	4.02	−2.55	1.5	2, 3[a]
BD +23°3130	5255	2.89	−2.42	1.7	6
BD +26°3578	6280	3.93	−2.25	2.0	2
BD −13°3442	6390	3.88	−2.66	1.4	3

References. — (1) Korn et al. (2003); (2) Gehren et al. (2006); (3) Mashonkina et al. (2008); (4) Tan et al. (2009); (5) determined with ELODIE spectra by this work; (6) determined with UVES spectra by this work.

[a] The average value adopted.

Table 2. Abundance results

Star	[O/H]	Ref.	$\log \epsilon$(Be)	Ref.	σ(Be)	$\log \epsilon$(B)	$\log \epsilon$(B) NLTE			σ(B)
	NLTE		LTE			LTE	$S_{\rm H} = 0$	$S_{\rm H} = 0.1$	$S_{\rm H} = 1$	
HD 19445	−1.40	8	−0.50	7	0.13	0.56	0.74	0.67	0.59	0.19
HD 64090	−1.08	2	−0.02	7	0.15	1.24	1.33	1.27	1.25	0.13
HD 76932	−0.43	11	0.88	7	0.14	2.03	2.08	2.07	2.05	0.14
HD 84937	−1.69	2	−0.85	7	0.12	< 0.43	< 0.73	< 0.72	< 0.55	···
HD 94028	−0.95	4	0.33	7	0.13	1.24	1.35	1.31	1.26	0.16
HD 106516	−0.30	1	< -0.58	5	···	1.38	1.45	1.43	1.41	0.15
HD 140283	−1.77	8	−0.96	7	0.14	0.07	0.27	0.18	0.11	0.22
HD 160617	−1.38	8	−0.41	12	0.12	0.51	0.66	0.62	0.55	0.20
HD 184499	−0.27	3	1.02	7	0.16	2.20	2.23	2.23	2.22	0.17
HD 194598	−0.77	11	0.18	7	0.14	1.38	1.46	1.44	1.40	0.14
HD 201891	−0.64	9	0.51	7	0.14	1.72	1.79	1.76	1.73	0.15
HD 221377	−0.63	1	< -0.92	3	···	1.41	1.50	1.50	1.48	0.19
BD +3°740	−2.16	2	−1.14	7	0.13	< 0.44	< 0.77	< 0.74	< 0.54	···
BD +23°3130	−1.66	4	−1.33	6	0.14	−0.18	−0.02	−0.12	−0.16	0.25
BD +26°3578	−1.73	8	−0.77	7	0.13	< 0.24	< 0.52	< 0.52	< 0.36	···
BD −13°3442	−2.22	10	−1.29	7	0.12	< 0.23	< 0.55	< 0.52	< 0.33	···

References. — (1) Sneden et al. (1979); (2) Tomkin et al. (1992); (3) Boesgaard & King (1993); (4) Cavallo et al. (1997); (5) Molaro et al. (1997); (6) García López et al. (1998); (7) Boesgaard et al. (1999); (8) Nissen et al. (2002); (9) Fulbright & Johnson (2003); (10) Akerman et al. (2004); (11) Jonsell et al. (2005); (12) Tan et al. (2009).

Table 3. Results of linear least-squares fits to the Be and B abundance data

x	y	Slope	Intercept
This work			
$\log\epsilon(\mathrm{Be})$	[Fe/H]	1.11 ± 0.10	1.74 ± 0.16
$\log\epsilon(\mathrm{B})_{\mathrm{LTE}}$	[Fe/H]	1.17 ± 0.13	2.96 ± 0.19
$\log\epsilon(\mathrm{B})_{\mathrm{NLTE,S_H=0}}$	[Fe/H]	1.07 ± 0.12	2.92 ± 0.19
$\log\epsilon(\mathrm{Be})$	[O/H]	1.33 ± 0.13	1.40 ± 0.14
$\log\epsilon(\mathrm{B})_{\mathrm{LTE}}$	[O/H]	1.46 ± 0.16	2.63 ± 0.17
$\log\epsilon(\mathrm{B})_{\mathrm{NLTE,S_H=0}}$	[O/H]	1.34 ± 0.15	2.62 ± 0.16
Rich & Boesgaard (2009)			
$\log\epsilon(\mathrm{Be})$	[Fe/H]	0.92 ± 0.04	1.41 ± 0.09
$\log\epsilon(\mathrm{Be})$	[O/H]	1.21 ± 0.08	1.32 ± 0.14
Tan et al. (2009)			
$\log\epsilon(\mathrm{Be})$	[Fe/H]	1.10 ± 0.07	1.63 ± 0.10
$\log\epsilon(\mathrm{Be})$	[O/H]	1.30 ± 0.08	1.19 ± 0.08
Smiljanic et al. (2009)			
$\log\epsilon(\mathrm{Be})$	[Fe/H]	1.24 ± 0.07	1.62 ± 0.08
$\log\epsilon(\mathrm{Be})$	[α/H]	1.36 ± 0.08	1.38 ± 0.07
Boesgaard et al. (1999)			
$\log\epsilon(\mathrm{Be})$	[Fe/H]	0.96 ± 0.04	1.41 ± 0.03
$\log\epsilon(\mathrm{Be})$	[O/H]	1.45 ± 0.04	1.31 ± 0.04
Duncan et al. (1997)			
$\log\epsilon(\mathrm{B})_{\mathrm{LTE}}$	[Fe/H]	0.96 ± 0.07	2.59 ± 0.13
$\log\epsilon(\mathrm{B})_{\mathrm{LTE}}$	[O/H]	1.21 ± 0.13	2.25 ± 0.16